*Plasma Processes and Polymers*

PLASMA PROCESSES AND POLYMERS

RESEARCH ARTICLE OPEN ACCESS

# Rapid Degradation of Aflatoxins by Treatment With Vacuum Ultraviolet Radiation Arising From Hydrogen Plasma

Nina Recek[1] | Dane Lojen[1] | Peter Gselman[2] | Rok Zaplotnik[1] | Gregor Primc[1] | Miran Mozetič[1]

[1]Department of Surface Engineering, Jozef Stefan Institute, Ljubljana, Slovenia | [2]Interkorn Ltd., Beltinci, Slovenia

**Correspondence:** Miran Mozetič (miran.mozetic@ijs.si)

**Received:** 4 September 2025 | **Revised:** 1 November 2025 | **Accepted:** 5 December 2025

**Funding:** This research was funded by the Slovenian Research Agency—research core funding No. P2-0082 (thin film structures and plasma surface engineering) and Project No. L7-4567 (plasma VUV and UV radiation–A method for successfully deactivating aflatoxins). The funders had no role in the design of the study; in the collection, analyses, or interpretation of data; in the writing of the manuscript; or in the decision to publish the results.

**Keywords:** aflatoxins | degradation | hydrogen plasma | maize | vacuum ultraviolet radiation

## ABSTRACT

A rapid, nonthermal method for surface decontamination of aflatoxins B1, G1, B2, and G2 was developed using vacuum ultraviolet (VUV) photons emitted from an inductively coupled hydrogen plasma. The plasma, sustained at 18 Pa with input powers between 50 and 700 W, produced intense VUV emission in the 140–160 nm range (photon energy ≈ 8 eV) that was delivered to samples through an $MgF_2$ window with > 80% transmittance. On quartz glass substrates coated with 40 ng of aflatoxin mix (film thickness ≈3 nm), VUV photons caused > 90% degradation within 10 s of VUV exposure. When applied to artificially contaminated maize grains (≈20 μg $kg^{-1}$ AFB1/G1, 4 μg $kg^{-1}$ AFB2/G2), VUV treatment achieved up to 80% toxin removal in under 1 min as measured by HPLC, but the remaining (≈20%) persisted even after 10 min of VUV irradiation, which was explained by the inability of VUV photons to penetrate into micron-scale grooves and crevices on the maize grain surface. These findings demonstrate that hydrogen-plasma VUV radiation can rapidly inactivate surface-bound aflatoxins on smooth substrates and agricultural commodities. However, the restricted penetration depth and vacuum chamber requirements limit bulk-grain scalability. Hybrid approaches combining VUV pretreatment with mechanical agitation and enzymatic degradation may offer a more energy-efficient, scalable solution for decontaminating porous food substrates.

## 1 | Introduction

Aflatoxins are aromatic organic compounds produced in minute quantities by several fungi in an adequate environment [1–3]. They are very toxic to humans and many animals [4, 5], and have also been proven to be carcinogenic [6–8]. Chronic exposure to aflatoxins leads to liver cancer, immunosuppression, and stunted growth in children, imposing severe public health burdens worldwide. Beyond health impacts, regulatory limits on aflatoxin levels trigger frequent crop rejections and trade barriers, resulting in annual economic losses in the agro-food industry estimated at over $1 billion globally [9, 10].

Aflatoxins are very stable compounds that cannot be degraded by boiling or applying any other standard method for destroying organic molecules. Roasting at a temperature of about 500 K causes slow degradation, but the technique is impractical for large-scale operations [11]. Some fungi cause the gradual degradation of aflatoxins in a biological environment [12]. Various methods for the degradation of aflatoxins have been reported in

**Abbreviations:** AFB1, aflatoxin B1; AFB2, aflatoxin B2; AFG1, aflatoxin G1; AFG2, aflatoxin G2; AF(s), aflatoxin(s); HPLC, high-performance liquid chromatography; RF, radiofrequency; SEM, scanning electron microscopy; UV, ultraviolet; VUV, vacuum ultraviolet.

the scientific literature. A classical one reported decades ago uses enzymes [13, 14]. Enzymatic degradation exploits laccases, peroxidases, and bacterial enzymes to selectively break down aflatoxin $B_1$, often producing less toxic metabolites [15]. Recently, Xu et al. [16] reported two peroxidase enzymes that proved better than the standard single-enzyme degradation. Despite specificity and mild reaction conditions, enzyme-based methods face challenges in terms of enzyme cost, stability, and integration into existing processing lines. None have been widely commercialised for grain decontamination [17]. However, the biological methods remain popular for the degradation of aflatoxins [18–20].

Singh et al. [21] suggested a proteinaceous pathway and found 80% degradation after 1-day incubation. Zhang et al. [22] employed microwave heating, while Chen et al. [23] employed photocatalytic treatment. Niu et al. [24] treated aflatoxins with X-rays and reported over 50% degradation when the dose of X-rays approached 10 kGy. The authors also reported possible degradation pathways. Wang et al. [25] treated aflatoxins with a low-pressure gaseous plasma sustained in the residual atmosphere at 15 Pa by capacitively coupled radio frequency (RF) discharge, while the application of atmospheric-pressure plasma was disclosed in [26]. The newest report on the application of gaseous plasma was provided by Nguyen et al. [27]. Other available techniques for the degradation of aflatoxins are reviewed in [28].

Irradiation of liquids containing aflatoxin with ultraviolet (UV) radiation was probably first mentioned in 1985, but details were not provided [29]. Liu et al. [30] also used UV radiation, but did not mention the type of UV source. Ultraviolet (UV) irradiation offers a non-chemical route to degrade aflatoxins in liquids and on surfaces. Reports date back to UV-C milk treatment for $M_1$ reduction and aqueous B1 degradation using low-pressure mercury lamps [29, 30]. Pulsed-light systems and LED-based UV-A reactors have shown up to 90% toxin removal in thin films and water matrices, while combined peroxide-UV treatments enhance degradation rates [31–33]. However, limited penetration depth and uneven exposure on grain surfaces constrain the scalability of this technique.

Aflatoxins exhibit fluorescence which peaks at the wavelength of ~428 nm for aflatoxin B1, ~425–430 nm for aflatoxin B2, ~450 nm for aflatoxin G1, and ~465 nm for aflatoxin G2 [34, 35].

The brief literature survey indicates that methods for aflatoxin degradation remain a hot scientific topic, probably because a technologically applicable method is yet to be invented. Namely, none of the methods reported in the scientific literature are scalable or enable degradation within a reasonable time.

We employed vacuum ultraviolet radiation (VUV) to destroy aflatoxins on the surface of model substrates and maize grains. The source of VUV radiation was low-pressure gaseous plasma. Most plasmas radiate in the VUV range [36], but we chose hydrogen plasma because it is the most efficient source of such radiation. Classical literature reports that up to about 10% of discharge power is transformed into VUV radiation [37], provided that the discharge power density (power spent on plasma excitation divided by the plasma volume) is large. Powerful plasma will cause significant heating of any product, so we isolated photochemistry from plasma-induced heating and reactive species with a VUV-transparent window. According to Wunderlich et al. [38], the transmission of $MgF_2$ windows for VUV radiation is above 0.8 down to the wavelength of about 200 nm. The transmittance decreases with decreasing wavelength and assumes values of 0.5 and 0.2 at 140 and 120 nm, respectively. The transmittance is marginal below 113 nm. We evaluated degradation kinetics on quartz substrates and maize grains, and analysed penetration constraints for the potential use of VUV-based plasma decontamination for agro-food safety.

## 2 | Experimental Details

Commercially available aflatoxins were purchased from Biopure (Romer Labs, Austria). The BiopureTM MIX contained a mixture of aflatoxins at concentrations of 2 μg/mL for Aflatoxin B1, 2 μg/mL for Aflatoxin G1, 0.5 μg/mL for Aflatoxin B2, and 0.5 μg/mL for Aflatoxin G2 in acetonitrile. The solution was applied to model substrates (quartz glass discs). Maize grains were artificially contaminated with an aflatoxin mix in a concentration of approximately 20 μg/kg for aflatoxin B1 and G1 and 4 μg/kg for B2 and G2 by dipping the grains into the mix solution.

### 2.1 | Experiments With Model Substrates

The BiopureTM MIX solution was deposited onto glass substrates. The substrates were discs of thickness 1 mm and diameter 4 mm made from quartz glass. They were purchased from Lianyungang Huoyunquartz Technology Co. Ltd., China. The discs were first cleaned in ethanol in an ultrasound bath before the deposition of the aflatoxin solution. Droplets of volume 2 μL were deposited on glass substrates. The surface tension of acetonitrile is low, so the droplet of the aflatoxin solution spreads rather uniformly on the entire glass surface. Acetonitrile has a high vapour pressure at room temperature, so the solvent evaporates within several minutes after being deposited on the glass surface. The aflatoxins remained on the surface after acetonitrile had evaporated. The mass of dry aflatoxins on the glass substrates was calculated from the droplet volume and the concentration of aflatoxins in the BiopureTM MIX. Since the concentration was 20 μg/mL and the droplet volume was 2 μL, the mass of dried toxins on the glass substrates was 40 ng. If the toxins were deposited in a laterally uniform film, the thickness would be about 3 nm.

The relative amount of aflatoxins on the glass substrates was determined by optical fluorescence. Namely, the aflatoxins used in this study exhibit natural fluorescence when illuminated with photons of appropriate wavelength. We used a multi-mode microplate reader (Tecan Infinite PRO 2000, Switzerland) to monitor the fluorescence. The samples were illuminated at an excitation wavelength of 230 nm, and emission wavelengths from 340 to 640 nm were measured. A standard calibration curve was prepared by measuring the fluorescence emission of aflatoxin mix at determined concentrations, as explained in [39]. Briefly, the original solution was diluted using high-purity acetonitrile and deposited onto glass substrates. The fluorescence was measured, and the intensity was plotted versus the concentration of aflatoxins in the deposited droplet. The equivalent toxin-film thickness was calculated based on the aflatoxin concentration that remained on the surface.

The quartz substrates coated with 40 ng of aflatoxin mix were treated with VUV radiation. The source of VUV radiation was a radiofrequency inductively coupled hydrogen plasma. The scheme of the experimental setup is shown in Figure 1. The discharge tube was made from a borosilicate glass tube with a diameter of 4 cm. A copper coil was fixed onto the discharge tube and connected to a radiofrequency generator (Cesar 1310, Advanced Energy, Fort Collins, CO, USA) via a matching network (Advanced Energy, Fort Collins, CO, USA). The discharge tube was pumped with a rotary pump with an ultimate pressure below 0.1 Pa and a nominal pumping speed of 80 $m^3$/h. Hydrogen of commercial purity 99.999% was leaked into the discharge tube during continuous pumping using a flow controller Aera FC-7700 (Advanced Energy, Denver, USA). The hydrogen flow of 70 sccm resulted in a pressure of 18 Pa. The pressure was measured with an absolute gauge (MKS Instruments, Andover, MA, USA). VUV spectra were acquired with a VS7550 V-UV to NIR Mini-Spectrograph (Resonance LTD., Canada). The position of the spectrometer is shown in Figure 1. The atmosphere in the discharge tube was separated from the photon detector with an $MgF_2$ window.

Numerous quartz glass substrates with the same amount of dry toxins (40 ng) were prepared. They were treated in the experimental system shown in Figure 1. Each substrate was covered with a VUV-transparent window except for the control samples, which were not mounted in the plasma chamber. We used magnesium difluoride windows supplied by Crystal GmbH, Berlin, Germany. The VUV-transparent window was fitted to the glass substrate, which was covered with a very thin film of dry aflatoxins, as shown in Figure 1. There was no loss of aflatoxins from the glass substrates because the contact with a VUV-transparent window was negligible.

Thermal effects are not the primary driver of aflatoxin degradation in plasma treatments [39]. The study concluded that the rapid degradation of aflatoxins during plasma treatment is predominantly due to reactions with oxygen plasma species, particularly neutral oxygen atoms, rather than elevated temperatures. Degradation of aflatoxins due to thermal effects from hydrogen plasma is therefore negligible.

## 2.2 | Experiments With Maize

Maize grains, hybrid 9241, were sterilised by autoclaving before the experiment. Some grains were pasted onto a sample holder and imaged by scanning electron microscopy (SEM). A typical SEM image of a grain surface is shown in Figure 2. The surface exhibits rich morphology with grooves and gaps.

Maize grains were dipped into the aflatoxin solution and then dried at ambient temperature. Afterwards, the grains were subjected to treatment with VUV radiation. We used an experimental setup shown in Figure 3. The source of VUV was an inductively coupled hydrogen plasma generated at 18 Pa. The discharge glass tube was 30 cm long with an inner diameter of 3.6 cm. The 6-turn excitation coil was connected to the RF generator (Advanced Energy CESAR 1320) via a matching network. The discharge chamber was pumped with a two-stage rotary vacuum pump (Trivac D40B Leybold). The discharge tube was vertically oriented, as shown in Figure 3. The sample chamber and the discharge chamber were separated with an $MgF_2$ VUV transparent window. The $MgF_2$ window was positioned 33 cm from the centre of the coil on the top of the sample chamber. Considering the $MgF_2$ window's diameter (4 cm) and its distance from the centre of the coil (33 cm), the utilisation of the irradiated VUV from plasma was about 0.1%. The only plasma-generated species that reached the samples were therefore photons. The sample chamber was vacuum-tight and was filled with nitrogen, so there was practically no VUV absorption above 130 nm. Namely, pure nitrogen does not absorb VUV photons in the photon energy range transmitted through a $MgF_2$ window, and the concentration of gaseous impurities (mainly oxygen and water vapour) was below 100 ppm. The absorption coefficient for oxygen in this range peaks at about 140 nm and is just above 300 $cm^{-1}$ at atmospheric pressure. This value was reported by several authors and confirmed in the classical literature by a carefully designed experiment, in which oxygen was irradiated with the VUV photons arising from hydrogen plasma [40]. Again, we must stress that plasma-generated ions and atoms did not reach the samples. Samples were treated only with UV and VUV emission. Each sample contained 10 g of maize grains. Grains were placed inside a sample chamber, as shown in Figure 3. The

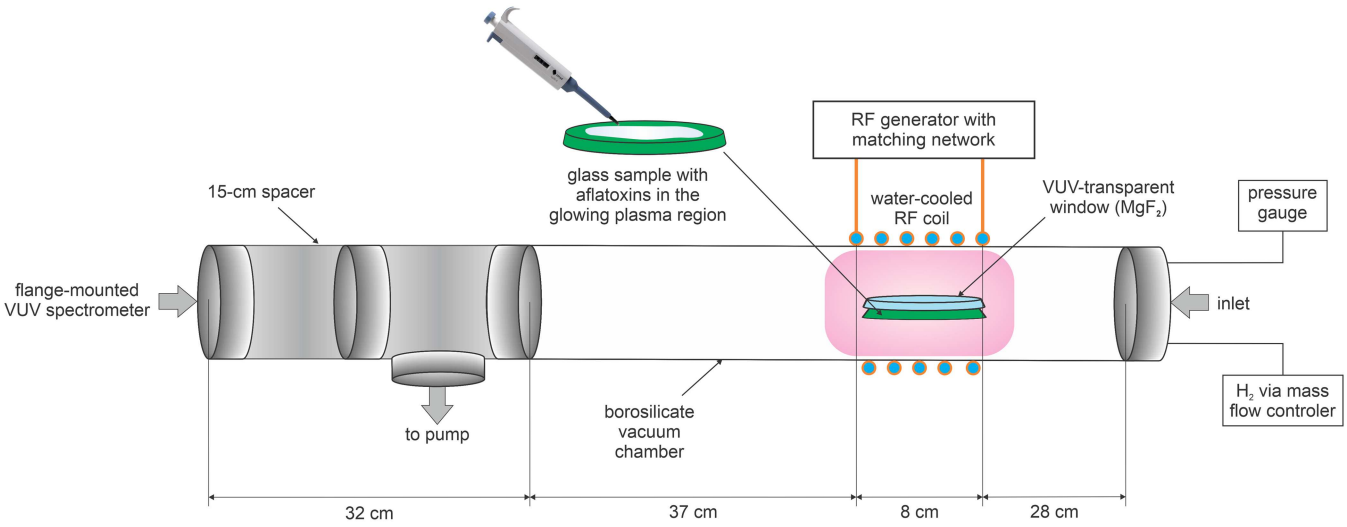


**FIGURE 1** | Schematic of the discharge chamber for treating samples with VUV radiation (not to scale).

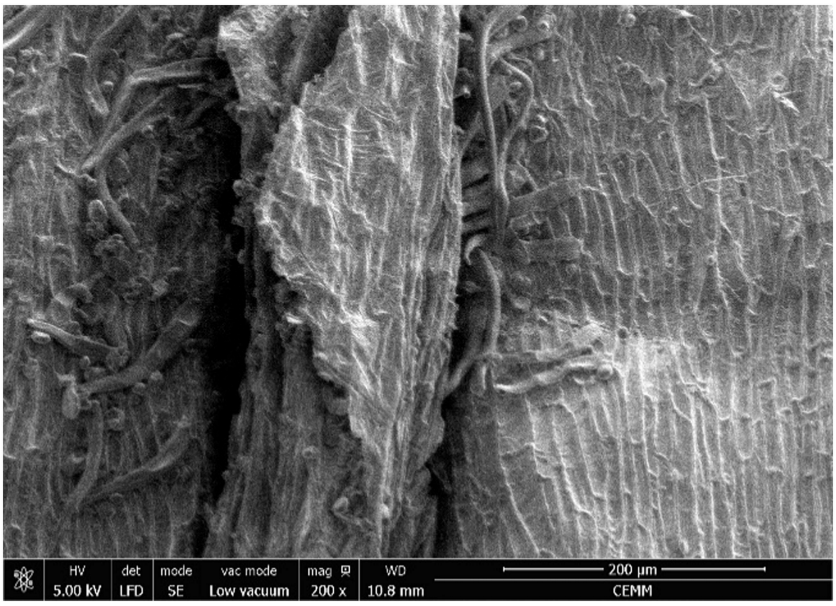


**FIGURE 2** | A typical image of the surface of a maize grain.

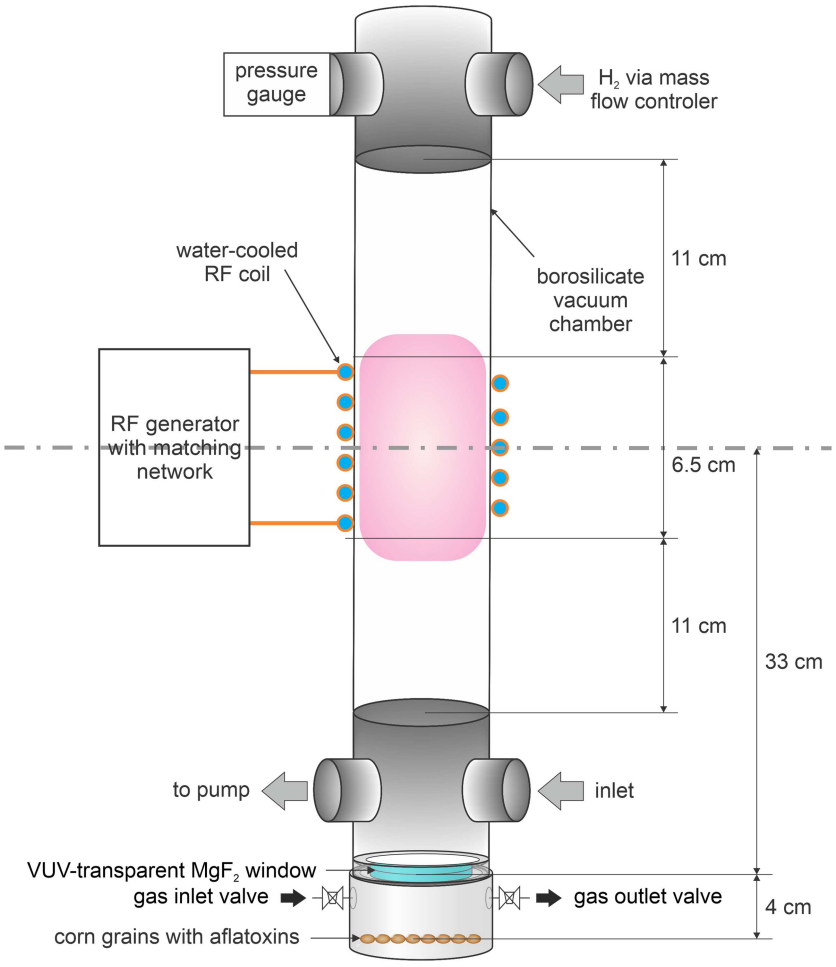


**FIGURE 3** | Experimental setup of VUV treatment of maize grains (not to scale).

treatment was pulsed, meaning there were time intervals between "plasma on" and "plasma off" treatments. During the "plasma-off" time, the entire plasma device system was manually moved from a vertical to a horizontal position and back three times, and then shaken, so that the grains were distributed relatively evenly in the sample chamber before the next "plasma on" interval. Such mixing enabled fairly uniform exposure of the entire grain surface to VUV radiation. The loss of

aflatoxins due to the chamber movement and mixing was negligible.

The concentration of aflatoxins on untreated and VUV-treated maize grains was measured by high-performance liquid chromatography (HPLC). For the preparation of maize with an aflatoxin B1 and G1 (AFB1 and AFG1) concentration of 0.020 mg/kg and aflatoxin B2 and G2 (AFB2 and AFG2) concentration of 0.005 mg/kg, 200 mL acetonitrile containing 7 μg AFB1 and AFG1, and 1.75 μg AFB2 and AFG2 (3.5 mL standard with AFB1 and AFG1 concentration of 2 μg/mL and AFB2 and AFG2 concentration of 0.5 μg/mL) was added to 350 g of uncontaminated maize grains (a sample of 10 g was analysed before treatment). The solution was evaporated at room temperature. The concentration of aflatoxins (AFs) was determined in two samples of contaminated maize (10 g each). Before the analysis, aflatoxins were extracted from the surface of treated maize seeds. The linear shaker IKA HS 501 digital (IKA Labortech-nik, Staufen, Germany) was used for the extraction. AFs were extracted from the samples with a mixture of methanol and deionised water (50 + 50). The extraction in all samples was performed on unground kernels.

We used a HPLC system (Waters Alliance 2690, Milford, MA, USA) equipped with a computer with Millennium program for the system control and data processing, a Phenomenex Prodigy column 5 μm ODS (2), 250 × 4.60 mm (Torrance, CA, USA), a Kobra cell (Rhone diagnostics, Glasgow, UK) for the post-column derivatisation with bromine and a Waters 474 scanning fluorescence detector.

The extract was cleaned up with immunoaffinity columns (R-Biopharm Rhone). AFs were eluted from the column with 1 mL of methanol. The column was then washed with 1 mL of deionised water, which was added to the eluate. AFs were determined by liquid chromatography with fluorescence detection (Waters) after derivatisation with bromine in a Kobra cell (Rhône diagnostics). The mobile phase was a mixture of deionised water, methanol, and acetonitrile (600 + 200 + 200), adding 350 μL of a 4 M $HNO_3$ solution and 119 mg KBr. The flow rate was 1 mL/min, the injection volume 100 μL, and the column temperature 30°C. The detection was performed at $\lambda_{Ex} = 362$ nm and $\lambda_{Em} = 425$ nm.

After treatment with VUV photons, the AF concentration was determined in each sample using the same HPLC-FLD procedure.

## 3 | Results and Discussion

### 3.1 | Aflatoxin Fluorescence

Figure 4a shows the fluorescence emission spectra of aflatoxin films deposited on a quartz glass substrate and excited at a wavelength of 230 nm. The emission intensity is plotted against wavelength, and the mass of deposited aflatoxins is varied as the key parameter (ranging from 0.4–40 ng). Each curve represents a distinct aflatoxin mass, with intensity increasing monotonically with mass.

The spectra display a clear fluorescence peak for the aflatoxin mix centred around 440 nm, and the intensity of this peak increases with the quantity of deposited toxin. The lowest-intensity curve corresponds to the mass of deposited aflatoxins of 0.4 ng, while the maximum intensity is observed for 40 ng. The baseline signal from the acetonitrile control (solvent only) is also included and remains barely visible, confirming negligible background fluorescence from the solvent.

The fairly linear increase in fluorescence with increasing aflatoxin mass, particularly within the range of 2–40 ng, supports the assumption of an optically thin film, where fluorescence intensity is directly proportional to toxin mass. These spectra are used to calibrate the fluorescence signal against toxin mass in subsequent plasma degradation experiments (Figure 4b).

### 3.2 | VUV Radiation From Hydrogen Plasma

Hydrogen plasma sustained at a pressure of 18 Pa was characterised with a VUV spectrometer. The acquired spectra for a few discharge powers are shown in Figure 5. As expected, the intensity increases with the increasing discharge power. The shape of the spectra, however, is very similar. Figure 5 shows intense radiation arising from the transitions of electronically highly excited states in the range of wavelengths between about 130 and 160 nm (photon energy between 9.5 and 7.8 eV). This transition arises from both the singlet and triplet systems of neutral hydrogen molecules (Werner and Lyman molecular bands) [37]. Furthermore, a well-pronounced continuum peaks at about 183 nm (photon energy 6.8 eV). The continuum expands toward the UV range and results from the radiative dissociation of highly excited neutral hydrogen molecules [37].

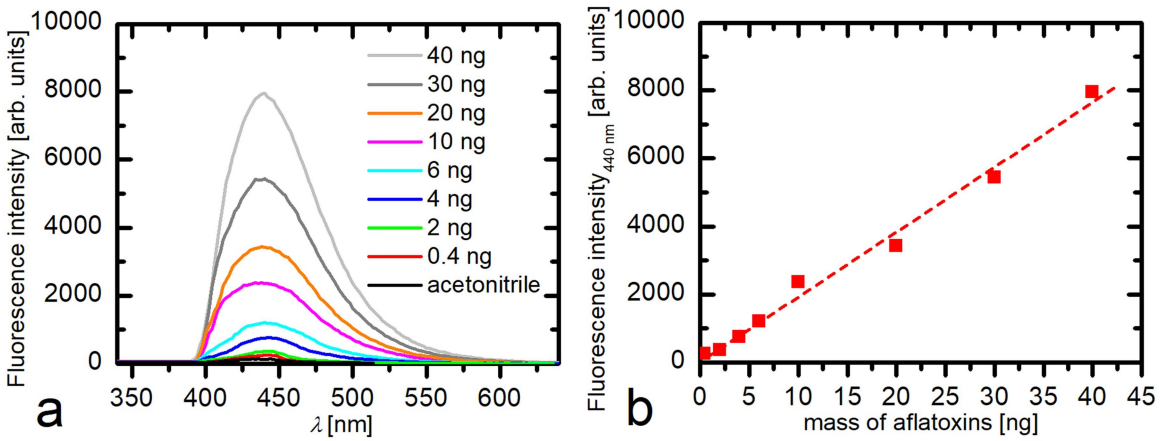


**FIGURE 4** | Fluorescence spectra of aflatoxin samples illuminated with 230 nm photons as a function of deposited toxin mass (a), and fluorescence intensity at 440 nm vs. mass of aflatoxins (b).

Photons with energies of 6–9 eV (≈140–206 nm) carry more than enough energy to overcome typical covalent bond dissociation thresholds (~3.5–4.5 eV) [41]. However, whether those photons actually break bonds in the aflatoxin molecule hinges on several photochemical factors: strong absorption at the photon wavelength, an allowed excited-state transition, and a photodissociation quantum yield high enough to compete with rapid nonradiative decay. In practice, aflatoxin B1 absorbs primarily below 300 nm and channels most excitation energy into ultrafast relaxation pathways, making direct bond breakage by 6–9 eV photons highly inefficient [31, 42, 43].

The penetration depth of photons in the VUV part of the spectrum is yet to be measured for aflatoxins, but as a rule of thumb, it decreases with increasing photon energy. For some organic molecules, it is about 100 and 1000 nm at the photon wavelength of 140 and 200 nm, respectively [44]. Since the thickness of the dried aflatoxins on the glass substrates is a few nm only, it is possible to conclude that the aflatoxin deposits are optically thin and that the photons in the low-wavelength part of the spectra in Figure 5 contribute more effectively to the aflatoxin degradation.

### 3.3 | Degradation of Toxins on Glass Substrates

The quartz glass substrates coated with a thin layer of aflatoxins and covered with a VUV-transparent window were treated with VUV radiation in the experimental system shown in Figure 1.

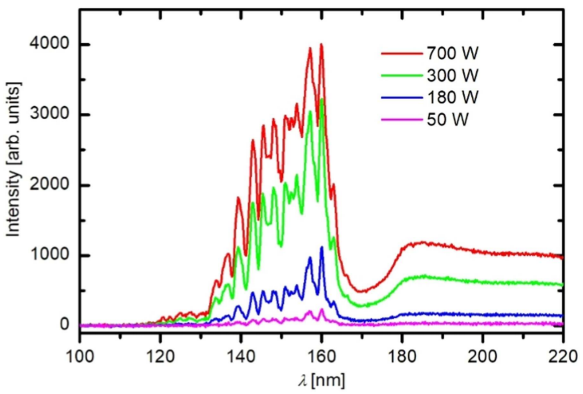


**FIGURE 5** | The radiation transmitted through the VUV-transparent window. The discharge power is the parameter.

Triplicates of the samples were treated simultaneously and probed by fluorescence spectrometry within half an hour after the treatment with the VUV radiation. The remaining mass of the aflatoxins versus the treatment time is shown in Figure 6. As expected, the mass of the remaining aflatoxin decreases with treatment time. The mass of remaining aflatoxins approaches the detection limit of fluorescence spectrometry after treating the samples for about 10 s.

It is not feasible to measure the flux of photons in our systems, but according to Fanz et al. [37], it should be of the order of $10^{20}\,m^{-2}\,s^{-1}$. The flux of VUV photons from low-pressure plasma depends on numerous parameters, and the major ones are the type of gas and the electron density. In the case of hydrogen plasma sustained at a pressure of several Pa, the flux of photons is similar to the flux of ions [37]. In fact, there is a direct correlation between the ion flux and the plasma density in low-pressure plasmas, that is, the flux increases almost linearly with increasing plasma density following the equation $j = k\,n$ [36]. Here, $j$ is the VUV photon flux, $n$ is the plasma density, and k is the coefficient deduced from over 20 various measurements. According to [36], the coefficient k is $3 \times 10^2$ m/s. Typical deviation from this general line is by a factor of 3 or 4 and depends mostly on the type of gas. The general line is valid only for low-pressure plasmas, which are optically thin, of course.

### 3.4 | Degradation of Toxins on Maize Grains

The experimental results shown in Figure 6 indicate rapid degradation of toxins deposited on model substrates. Based on these results, we selected different treatment times to measure the degradation of toxins on maize grains. We selected different discharge powers and various treatment times. The results are presented in Figure 7. We used HPLC to measure the concentration of aflatoxins in the whole grains extracted from the sample surface. The HPLC spectra of the analysed samples can be found in the open repository Zenodo (https://doi.org/10.5281/zenodo.17358345).

Fluorescence detection limit (100 μL, 96-well plate) on the Tecan Infinite 200 PRO is approximately $7 \times 10^{-16}$ mol, corresponding to ~$4 \times 10^8$ molecules per well. In our experiments, the mass of aflatoxins ranged from 0.4–40 ng, corresponding to approximately $1.28 \times 10^{-10}$ and $1.28 \times 10^{-12}$ mol, respectively,

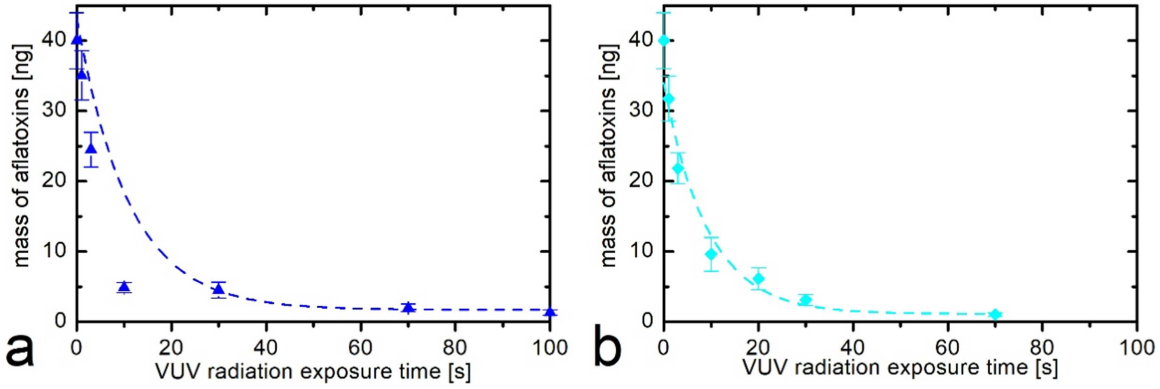


**FIGURE 6** | The mass of aflatoxins on a quartz glass substrate after treatment with VUV radiation from hydrogen plasma at various VUV exposure times. (a) at discharge power 300 W, and (b) 700 W.

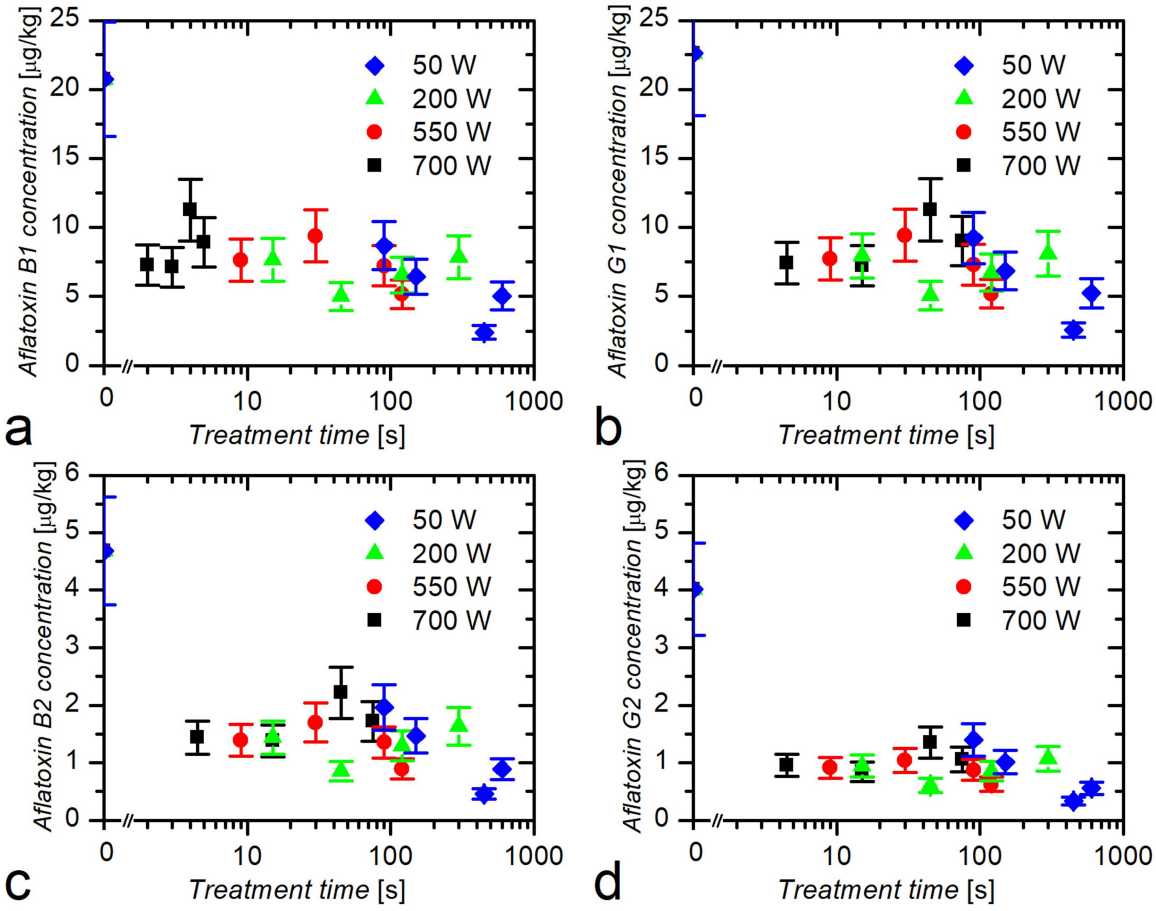


**FIGURE 7** | Aflatoxin concentration on the maize grains versus VUV radiation exposure time for (a) aflatoxin B1, (b) aflatoxin G1, (c) aflatoxin B2, and (d) aflatoxin G2. Aflatoxin concentration on the grains was determined with HPLC analysis, and duplicates for each sample were tested.

meaning the detection of the aflatoxins in solution was not questionable.

First observation is that the concentration of toxins on the untreated samples is rather small, that is, around 10 µg per kg of grains. Let us calculate the thickness of the aflatoxins on the grain surface in the approximation of a smooth surface. This approximation is not justified, taking into account the rich morphology as shown in Figure 2, but it is useful for estimating the maximal possible thickness. The thickness is

$$X = c\ m/(\rho\ S) \tag{1}$$

Here, $c$ is the measured concentration of aflatoxins, $m$ is the measured mass of a grain, $\rho$ is the density of toxins, and $S$ is the surface of a grain. Different grains had different masses, but the average was 0.25 g. Also, the surface of grains varied, but the average was $2 \times 10^{-4}\,\mathrm{m}^2$. Considering numerical values, the thickness of the deposited film of aflatoxins is about $x = 0.025$ nm. This value is well below the thickness of a monolayer of any material, so the simple calculation shows that the aflatoxin was unevenly distributed on the maize grains after dipping in the solution. Still, even such small concentrations are measurable by HPLC, with detection limit a few nanograms for many compounds. The following observation upon examining the results shown in Figure 7 is that the ratio of concentration of different toxins on the surface of the untreated sample is similar to that of the concentration in the original mix (i.e., 2:0.5). This observation clearly shows that the adsorption upon dipping grains in the aflatoxin mix is not selective.

The curves in different diagrams in Figure 7 are similar: the concentration of aflatoxins drops quickly upon treatment with VUV radiation, stabilising at about 20% of the initially deposited amount. This observation is not supported by Figure 6, which clearly shows complete degradation after prolonged treatment times. The discrepancy could be explained by the morphology of the maize grains (Figure 2). According to this explanation, the toxins are relatively uniformly distributed on the entire surface, including gaps, pores, grooves, and similar features. Namely, acetonitrile is a polar solvent, and its surface tension is much lower than the surface energy of maize grains. The liquid thus penetrates inside the morphological features. Once dried, the aflatoxins will remain inside the gaps. The VUV radiation quickly degrades the aflatoxins on the exposed surface of the grains, but cannot penetrate the gaps because their penetration depth in organic matter is much smaller than the depth of the gaps, grooves, etc. [45]. Therefore, the aflatoxins inside these morphological features remain intact even after prolonged treatment, up to 10 min, which was the longest treatment time used in our experiments.

The aflatoxin degradation products are not cytotoxic. In the study, Stanley et al. [32] demonstrated that UV-A irradiation at

365 nm effectively degraded aflatoxins B1 (AFB1) and M1 (AFM1) in ultrapure water, and the resulting degradation products were found to be less toxic than the parent compounds. Cytotoxicity analysis using HepG2 liver cells showed increased cell viability as the UV-A dose increased, with no significant cytotoxicity observed at the maximum dose of 1200 mJ/cm$^2$. This indicates that the degradation products are safe and do not adversely affect cell viability.

## 4 | Conclusions

The experiments performed on the model substrate clearly show that VUV radiation from hydrogen plasma effectively decomposes aflatoxins. The degradation of 40 ng of aflatoxin mix on a substrate with an area of about 1 cm$^2$ is accomplished after a few 10 s of exposure to radiation, whose source is hydrogen plasma sustained by an inductively coupled RF discharge at a power of several 100 W and pressure of 18 Pa. Plasma coupling at such conditions in the glass discharge chamber with an inner diameter of 3.6 cm is in the H-mode. The energy efficiency of such a system is rather low, since only roughly 10% of the RF discharge power is converted into useful VUV photons, which then contribute to molecular bond breaking. The remaining energy is lost to the system heating. The optimisation of VUV conversion efficiency will be essential to reduce the energy per mass of toxin degraded. However, even the most optimal UV plasma sources (low-pressure mercury lamps) do not exceed the energy efficiency of 20–30%. The lifetime of our plasma source, however, is very long because hydrogen plasma does not cause detectable modification of plasma-facing components. The scalability of such a process is constrained by the size of the vacuum chamber. The treatment uniformity may be questionable in any attempt to upscale the methods. Also, as shown in this paper, the aflatoxins in deep pores and surface crevices will remain inaccessible to VUV alone, so they persist even after prolonged irradiation with VUV photons. Because of these challenges, degradation with VUV photons from plasma is most suitable for decontaminating smooth flat surfaces—such as food packaging, and toxins on the surface of treated materials. For bulk agro-food commodities, hybrid solutions that combine VUV pretreatment with mechanical cleaning, enzymatic breakdown, or other decontamination steps may offer a more energy-efficient, scalable path forward.

### Author Contributions

Conceptualization by Nina Recek and Miran Mozetič. Methodology by Nina Recek, Rok Zaplotnik. Validation by Gregor Primc, Peter Gselman, Rok Zaplotnik, and Nina Recek. Interpretation by Miran Mozetič. Resources by Nina Recek, Miran Mozetič, and Peter Gselman. Data curation by Gregor Primc and Miran Mozetič. Writing – original draft preparation by Nina Recek. Writing – review and editing by Miran Mozetič, Gregor Primc. Visualization by Peter Gselman. Project administration by Nina Recek. Funding acquisition by Nina Recek and Miran Mozetič. All authors have read and agreed to the published version of the manuscript.

### Acknowledgements

Irena Ardalič from the Veterinary faculty, University of Ljubljana, is gratefully acknowledged for routine HPLC measurements, and Dr. Gabrijela Tavčar Kalcher from the Veterinary Faculty, University of Ljubljana, for guidance and discussion of the HPLC measurements.

### Conflicts of Interest

The authors declare no conflicts of interest.

### Data Availability Statement

The original data presented in the study are openly available in the repository Zenodo at https://doi.org/10.5281/zenodo.17358345.

### References

1. A. E. De Jesus, C. P. Gorst-Allman, R. M. Horak, and R. Vleggaar, "Large-Scale Purification of the Mycotoxins Aflatoxin B1, B2 and G1," *Journal of Chromatography A* 450 (1988): 101–104.

2. C.-M. Chang and J. Q. Lynd, "Soil Microfloral Interactions With Aflatoxin Synthesis and Degradation," *Mycologia* 62 (1970): 978–986.

3. M. F. Dutton, K. Ehrlich, and J. W. Bennett, "Biosynthetic Relationship Among Aflatoxins B1, B2, M1, and M2," *Applied and Environmental Microbiology* 49 (1985): 1392–1395, https://doi.org/10.1128/aem.49.6.1392-1395.1985.

4. C. Lovelace, H. Njapau, L. Salter, and A. Bayley, "Screening Method for the Detection of Aflatoxin and Metabolites in Human Urine: Aflatoxins B1, G1, M1, B2a, G2a, aflatoxicols I and II," *Journal of Chromatography B: Biomedical Sciences and Applications* 227 (1982): 256–261.

5. D. Veselý, D. Veselá, and R. Jelínek, "Comparative Assessment of the Aflatoxin B1, B2, G1, G2 and M1 Embryotoxicity in the Chick Embryo," *Toxicology Letters* 15 (1983): 297–300.

6. G. C. Onyemelukwe, G. H. Ogbadu, and A. Salifu, "Aflatoxins, B1, B2, G1, G2 in Primary Liver Cell Carcinoma," *Toxicology Letters* 10 (1982): 309–312.

7. A. Y. Nassar, S. E. Megalla, H. M. Abd El-Fattah, A. H. Hafez, and T. S. El-Deap, "Binding of Aflatoxin B 1, G 1 and M to Plasma Albumin," *Mycopathologia* 79 (1982): 35–38.

8. I. E. Yates, "Cytotoxicity and Mutagenicity of Aflatoxins B1, B2, G1 and G2 in Photobacterium Phosphoreum," *Journal of Microbiological Methods* 3 (1985): 181–186.

9. S. Shabeer, S. Asad, A. Jamal, and A. Ali, "Aflatoxin Contamination, Its Impact and Management Strategies: An Updated Review," *Toxins* 14 (2022): 307.

10. A. Jallow, H. Xie, X. Tang, Z. Qi, and P. Li, "Worldwide Aflatoxin Contamination of Agricultural Products and Foods: From Occurrence to Control," *Comprehensive Reviews in Food Science and Food Safety* 20 (2021): 2332–2381.

11. L. M. Martins, A. S. Sant'Ana, B. T. Iamanaka, M. I. Berto, J. I. Pitt, and M. H. Taniwaki, "Kinetics of Aflatoxin Degradation During Peanut Roasting," *Food Research International* 97 (2017): 178–183.

12. T. Shantha, "Fungal Degradation of Aflatoxin B1," *Natural Toxins* 7 (1999): 175–178.

13. J. F. Alberts, W. C. A. Gelderblom, A. Botha, and W. H. Van Zyl, "Degradation of Aflatoxin B1 by Fungal Laccase Enzymes," *International Journal of Food Microbiology* 135 (2009): 47–52.

14. J. F. Alberts, Y. Engelbrecht, P. S. Steyn, W. H. Holzapfel, and W. H. Van Zyl, "Biological Degradation of Aflatoxin B1 by Rhodococcus Erythropolis Cultures," *International Journal of Food Microbiology* 109 (2006): 121–126.

15. I. Dini, V. Alborino, S. Lanzuise, et al., "Trichoderma Enzymes for Degradation of Aflatoxin B1 and Ochratoxin A," *Molecules* 27 (2022): 3959.

16. X. Xu, P. Lin, Y. Lu, and R. Jia, "Degradation and Detoxification of Aflatoxin B1 by Two Peroxidase Enzymes From Irpex Lacteus F17," *Bioprocess and Biosystems Engineering* 48 (2025): 693–704.

17. Y. Guan, J. Chen, E. Nepovimova, M. Long, W. Wu, and K. Kuca, "Aflatoxin Detoxification Using Microorganisms and Enzymes," *Toxins* 13 (2021): 46.

18. A. Zapaśnik, M. Bryła, A. Wojtczak, and B. Sokołowska, "In Vivo Effectiveness of *Pleurotus ostreatus* in Degradation of Toxic Metabolites of Filamentous Fungi Such as Aflatoxin B1 and Zearalenone," *Metabolites* 15 (2025): 20.

19. J. Wang, J. Nan, Q. Chen, Y. Zhou, X. Gao, and Y. Li, "Exploration of Aflatoxin B1 Degradation Products via *Kocuria rosea*: Structure Elucidation and Toxicity Analysis," *Applied Sciences* 14 (2024): 11024.

20. T. Maneeboon, C. Roopkham, W. Mahakarnchanakul, and C. Chuaysrinule, "Exploration of *Pseudomonas knackmussii* AD02 for the Biological Mitigation of Post-Harvest Aflatoxin Contamination: Characterization and Degradation Mechanism," *Journal of Stored Products Research* 109 (2024): 102470.

21. J. Singh and A. Mehta, "Protein-Mediated Degradation of Aflatoxin B 1 by *Pseudomonas putida*," *Brazilian Journal of Microbiology* 50 (2019): 1031–1039.

22. Y. Zhang, L. Zhang, X. Zhang, et al., "Degradation of Aflatoxin B1 in Corn by Water-Assisted Microwave Irradiation and Its Kinetic," *Toxicon* 255 (2025): 108239.

23. S. Chen, H. Wang, Z. Mo, et al., "Highly Efficient g-C3N5/Bi2MoO6 Heterojunction for Aflatoxin B1 Photocatalytic Degradation," *Inorganic Chemistry Communications* 170 (2024): 113156.

24. J. Niu, Y. Li, Y. Deng, et al., "Degradation of Aflatoxin B1 by X-Ray Irradiation," *LWT* 217 (2025): 117384.

25. S.-Q. Wang, G.-Q. Huang, Y.-P. Li, J.-X. Xiao, Y. Zhang, and W.-L. Jiang, "Degradation of Aflatoxin $B_1$ by Low-Temperature Radio Frequency Plasma and Degradation Product Elucidation," *European Food Research and Technology* 241 (2015): 103–113, https://doi.org/10.1007/s00217-015-2439-5.

26. N. Nikmaram and K. M. Keener, "Aflatoxin M1 Degradation Using High Voltage Atmospheric Cold Plasma (HVACP) Technology," *Ozone: Science & Engineering* 45 (2023): 503–515.

27. T. Nguyen, J. Palmer, J. Pedley, et al., "The Effect of Variations in Cold Plasma Conditions on the Detoxification of Aflatoxin M1 and Degradation Products," *International Dairy Journal* 160 (2025): 106103, https://doi.org/10.1016/j.idairyj.2024.106103.

28. K. Kutasi, N. Recek, R. Zaplotnik, et al., "Approaches to Inactivating Aflatoxins-A Review and Challenges," *International Journal of Molecular Sciences* 22 (2021): 13322, https://doi.org/10.3390/ijms222413322.

29. A. E. Yousef and E. H. Marth, "Degradation of Aflatoxin M1 in Milk by Ultraviolet Energy," *Journal of Food Protection* 48 (1985): 697–698.

30. R. Liu, M. Chang, Q. Jin, J. Huang, Y. Liu, and X. Wang, "Degradation of Aflatoxin $B_1$ in Aqueous Medium Through UV Irradiation," *European Food Research and Technology* 233 (2011): 1007–1012.

31. B. Wang, N. E. Mahoney, R. Khir, et al., "Degradation Kinetics of Aflatoxin B1 and B2 in Solid Medium by Using Pulsed Light Irradiation," *Journal of the Science of Food and Agriculture* 98 (2018): 5220–5224.

32. J. Stanley, A. Patras, B. Pendyala, M. J. Vergne, and R. R. Bansode, "Performance of a UV-A LED System for Degradation of Aflatoxins B1 and M1 in Pure Water: Kinetics and Cytotoxicity Study," *Scientific Reports* 10 (2020): 13473.

33. M.-H. Shen and R. K. Singh, "Detoxification of Aflatoxins in Foods by Ultraviolet Irradiation, Hydrogen Peroxide, and Their Combination-A Review," *LWT* 142 (2021): 110986.

34. D. Bartolić, D. Mutavdžić, J. M. Carstensen, et al., "Fluorescence Spectroscopy and Multispectral Imaging for Fingerprinting of Aflatoxin-B1 Contaminated (*Zea mays* L.) Seeds: A Preliminary Study," *Scientific Reports* 12 (2022): 4849.

35. M. Chen, X. He, Y. Pang, F. Shen, Y. Fang, and Q. Hu, "Laser Induced Fluorescence Spectroscopy for Detection of Aflatoxin $B_1$ Contamination in Peanut Oil," *Journal of Food Measurement and Characterization* 15 (2021): 2231–2239.

36. D. Popović, M. Mozetič, A. Vesel, G. Primc, and R. Zaplotnik, "Review on Vacuum Ultraviolet Generation in Low-Pressure Plasmas," *Plasma Processes and Polymers* 18 (2021): 2100061, https://doi.org/10.1002/ppap.202100061.

37. U. Fantz, S. Briefi, D. Rauner, and D. Wünderlich, "Quantification of the VUV Radiation in Low Pressure Hydrogen and Nitrogen Plasmas," *Plasma Sources Science and Technology* 25 (2016): 045006.

38. D. Wünderlich, S. Briefi, R. Friedl, and U. Fantz, "Emission Spectroscopy of Negative Hydrogen Ion Sources: From VUV to IR," *Review of Scientific Instruments* 92 (2021): 123510.

39. N. Recek, R. Zaplotnik, G. Primc, P. Gselman, and M. Mozetič, "Low-Temperature Degradation of Aflatoxins via Oxygen Plasma: Kinetics and Mechanism Driven by Atomic Oxygen Flux," *Materials* 18 (2025): 2924.

40. K. Watanabe, E. C. Y. Inn, and M. Zelikoff, "Absorption Coefficients of Oxygen in the Vacuum Ultraviolet," *Journal of Chemical Physics* 21 (1953): 1026–1030.

41. Y. Liu, Y. Li, Q. Yang, J.-D. Yang, L. Zhang, and S. Luo, "Prediction of Bond Dissociation Energy for Organic Molecules Based on a Machine-Learning Approach," *Chinese Journal of Chemistry* 42 (2024): 1967–1974, https://doi.org/10.1002/cjoc.202400049.

42. N. J. Turro, V. Ramamurthy, and J. C. Scaiano, *Principles of Molecular Photochemistry: An Introduction* (University Science Books, 2009).

43. Z. Liu, H. Zhao, G. Yang, et al., "Study of Photodegradation Kinetics of Aflatoxins in Cereals Using Trilinear Component Modeling of Excitation-Emission Matrix Fluorescence Data," *Spectrochimica Acta, Part A: Molecular and Biomolecular Spectroscopy* 235 (2020): 118266.

44. M. Fouchier, E. Pargon, L. Azarnouche, et al., "Vacuum Ultra Violet Absorption Spectroscopy of 193 nm Photoresists," *Applied Physics A* 105 (2011): 399–405, https://doi.org/10.1007/s00339-011-6553-3.

45. M.-H. Shen and R. K. Singh, "Detoxification of Aflatoxins in Foods by Ultraviolet Irradiation, Hydrogen Peroxide, and Their Combination—A Review," *LWT* 142 (2021): 110986, https://doi.org/10.1016/j.lwt.2021.110986.